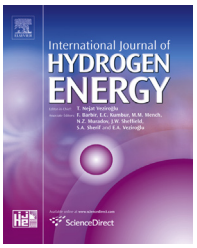
INTERNATIONAL JOURNAL OF HYDROGEN ENERGY XXX (2016) 1–9



Available online at www.sciencedirect.com

ScienceDirect

journal homepage: www.elsevier.com/locate/he



High performance solid-oxide fuel cell: Opening windows to low temperature application

Ye Zhang-Steenwinkel [a], Qingchun Yu [b], Frans P.F. van Berkel [a], Marc M.A. van Tuel [a], Bert Rietveld [a], Hengyong Tu [b,*]

[a] Energy Research Centre of the Netherlands (ECN), Westerduinweg 3, 1755 ZG, Petten, The Netherlands
[b] Institute of Fuel Cell, School of Mechanical Engineering, Shanghai Jiao Tong University, Shanghai, 200240, PR China

ARTICLE INFO

Article history:
Received 8 December 2015
Received in revised form
10 February 2016
Accepted 10 February 2016
Available online xxx

Keywords:
Low temperature SOFC
Zirconia based electrolyte
$La_{0.6}Sr_{0.4}CoO_{3-\delta}$ perovskite
Physical vapour deposition (PVD)
Screen printing (SP)
Cell performance

ABSTRACT

A key hindrance of operating solid oxide fuel cells (SOFCs) at low temperature is the relatively high cell resistance resulting in low power output density. In this work, we report an SOFC design based on an anode-supported cell (ASC) with thin film Yttria stabilized zirconia electrolyte (YSZ), capable of high power output densities of 1050 mW cm^{-2} using H_2 as fuel, at an operating temperature of 873 K. Such high cell performances have been realized by applying three optimization steps: (1) using $La_{0.6}Sr_{0.4}CoO_{3-\delta}$-perovskite (LSC) as high performing cathode material at low temperature; (2) integration of an optimized $Ce_{0.8}Gd_{0.2}O_{1.9}$ (CGO) inter-diffusion barrier layer and (3) optimization of the microstructure of the anode substrate by means of increasing the substrate porosity.

Copyright © 2016, Hydrogen Energy Publications, LLC. Published by Elsevier Ltd. All rights reserved.

Introduction

The Solid Oxide Fuel Cell (SOFC) is an attractive power generation device that directly and efficiently converts chemical energy from hydrogen or fossil fuels to electric power. Hence, this device combines the benefits of environmentally benign power generation with fuel flexibility [1,2]. However, the necessity to operate a conventional SOFC at high operating temperature (>1073 K) results in high costs of applied materials, especially the metallic interconnect and balance-of-plant materials, and material compatibility challenges [3,4]. The reduction of the operating temperature of SOFCs (823–923 K) is an effective approach for reducing the costs of applied materials and increasing lifetime of SOFCs [5,6].

Although it is well-known that the anode-supported cell (ASC) with thin film electrolyte is the most promising cell design for low temperature application [7,8], the performance of this type of cells at lower temperatures strongly declines due to rapidly increasing cathode polarisation losses [9,10]. The catalytic oxygen reduction activity of the currently used cathode materials like $(La, Sr)_{(1-x)}MnO_{3-\delta}$ and $(La,Sr)_{(1-x)}(Fe, Co)O_{3-\delta}$ is rather low for operation below 973 K [11–13]. In the literature, $La_{0.6}Sr_{0.4}CoO_{3-\delta}$ perovskite (LSC) has been proposed as cathode material for low-temperature SOFCs. This compound with rhombohedrally distorted perovskite structure is a well-known mixed ionic and electronic conducting material

* Corresponding author.
E-mail address: hytu@sjtu.edu.cn (H. Tu).

http://dx.doi.org/10.1016/j.ijhydene.2016.02.033

0360-3199/Copyright © 2016, Hydrogen Energy Publications, LLC. Published by Elsevier Ltd. All rights reserved.

Please cite this article in press as: Zhang-Steenwinkel Y, et al., High performance solid-oxide fuel cell: Opening windows to low temperature application, International Journal of Hydrogen Energy (2016), http://dx.doi.org/10.1016/j.ijhydene.2016.02.033

(MIEC) with high catalytic activity for oxygen reduction at low temperatures [14–16]. Another advantage of LSC as cathode is its high tolerance towards CO_2 in the desired temperature regime. That aspect makes LSC a more favourable low temperature cathode material than the highly promising $Ba_{0.5}Sr_{0.5}Co_{0.8}Fe_{0.2}O_{3-\delta}$ (BSCF), which has been demonstrated as good low temperature cathode but has low CO_2-tolerance [17,18]. A drawback of the use of LSC is the reactivity with YSZ electrolyte resulting in the formation of $SrZrO_3$, especially during the SOFC manufacturing procedure, involving sintering temperatures for the cathode as high as 1173–1373 K. $SrZrO_3$ has very poor oxygen ionic conductivity, leading to lower cell performance [12]. Therefore, a diffusion barrier layer between the YSZ electrolyte and LSC cathode is needed in order to prevent Sr diffusion from the cathode to the zirconia electrolyte. From the literature, $Ce_{0.8}Gd_{0.2}O_{1.9}$ (CGO) has been found to be a more suitable blocking layer, compared to $Ce_{0.8}Y_{0.2}O_{1.9}$ (CYO), due to its high ionic conductivity and chemical compatibility with the LSC-cathode along with low reactivity with Sr-containing cathode [7,19]. This ceria interdiffusion barrier layer needs to fulfil three requirements. First, this layer has to be thin resulting in the reduction of the ohmic contribution. Second, the ceria barrier layer has to be sintered at temperatures as low as possible in order to prevent interdiffusion of cations between the ceria and zirconia layer, which creates an undesirable reaction zone with a lower ionic conductivity that results in enhanced ohmic losses [8,20]. Third, this layer must be dense in order to prevent any reaction between cathode and zirconia electrolyte. Two techniques have been explored for the optimization of applied CGO layers in order to achieve those requirements, namely the cost efficient screen-printing technique (SP) and physical vapour deposition technology (PVD). The ceria deposition procedure using PVD has been demonstrated already to be a suitable technique with respect to those requirements [21]. This technique has the advantage of lowering the deposition temperature of the CGO layer to 1073 K or even below, which prevents the interdiffusion between CGO and YSZ.

The anode substrates used in Anode Supported Cells (ASC) are usually fabricated by tape casting method. The investigation of Ni-YSZ cermet anode indicated that the anode substrate structure can significantly influence the performance of the fuel oxidation reaction. Increasing porosity and pore size will allow for high electrochemical activity and less hindered gas transport [22,23].

In the present work, the significant improved cell performance at 873 K has been achieved by the use of LSC as cathode and improvement of quality of CGO interdiffusion barrier layer. The final improvement of cell performance has been obtained by optimization of the anode substrate with respect to porosity and pore size distribution.

Experimental

Fabrication of anode-electrolyte support

NiO (MERK), 3 mol% YSZ (TOSOH) and pore-former powder obtained from commercial sources were mixed into a tape cast suspension, consisting of PVB binder dissolved in ethanol-toluene mixture. After tape-casting and evaporation of the dispersion aid, the resulting green tape was cut in the appropriate dimension and the functional anode layer and electrolyte layer were applied by screen printing (200 mesh). The functional anode layer is prepared from a mixture of NiO (MERK) and 8 mol% YSZ ($Zr_{0.84}Y_{0.16}O_{1.92}$, TOSOH), powder from commercial sources. The electrolyte layer consists of 8 mol% YSZ. The screen print pastes were prepared by mixing these powders into a dispersant aid and binder system using a Dispermat milling device. The resulting green anode electrolyte support was sintered at 1673 K for 1 h. The sintered anode-electrolyte support consists of an approximately 550 μm thick anode substrate, an 8 μm thick electrochemical active anode functional layer and a 3–5 μm thick electrolyte layer. The state-of-the-art anode electrolyte support used as a reference to monitor the improvement in cell performance consists of an anode substrate supporting a bi-layer electrolyte of 8YSZ (4–5 μm) and $Ce_{0.8}Y_{0.2}O_{1.9}$, (CYO, 3–4 μm) that has been co-fired at 1673 K together with the anode substrate.

Preparation of ceria diffusion barrier layer

$Ce_{0.8}Gd_{0.2}O_{1.9}$ powder (CGO, from Rhodia) has been used for the ceria barrier layer development by means of screen printing technique (SP). Screen printing pastes have been prepared by mixing CGO powders into a dispersant aid and binder system using a Dispermat milling system. The pastes with additional sintering aid (cobalt nitrate salt, 0.6 mol dm^{-3}), aiming for dense and crack-free CGO layer after sintering, has been screen-printed onto the 5 × 5 cm^2 square-shaped anode-electrolyte support, followed by sintering at 1573 K. This sintering temperature has been found to be the most optimum one in our previous work. After the cell performance test, the microstructure and elemental composition of the CGO layer have been investigated by SEM (JEOL HSM-6330F Field Emissions Scanning Electron Microscope) equipped with an EDX spectrometer (Thermo Noran) on the cross section of the samples. Line-scans of the cross section of the tested samples were performed to determine the element distribution across the different layers. For the CGO layer prepared by PVD, the reactive sputtering technique was used. Therefore, a metallic alloy with a nominal composition of 80 at.% Ce and 20 at.% Gd has been sputtered in an argon/oxygen atmosphere with an oxygen partial pressure of 10^{-3} mbar.

Cathode manufacturing

The $La_{0.6}Sr_{0.4}CoO_{3-\delta}$ (LSC) screen printing pastes have been prepared by mixing the LSC powders (Praxair) into a dispersant aid and binder system using a Dispermat milling device. The resulting pastes have been screen-printed (SP) on top of the 5 × 5 cm^2 square shaped anode substrate support covered with either CGO or CYO layer. This LSC cathode has been first optimized for its electrochemical performance through microstructural modification by means of optimization of sintering step, aiming for sufficiently and uniformly small particles along with high catalytic oxygen reduction activity and well established particle-to-particle connectivity. The optimum sintering temperature has been determined to be

Please cite this article in press as: Zhang-Steenwinkel Y, et al., High performance solid-oxide fuel cell: Opening windows to low temperature application, International Journal of Hydrogen Energy (2016), http://dx.doi.org/10.1016/j.ijhydene.2016.02.033

1273 K resulting in the desirable cathode microstructure consisting of uniform and well connected cathode particles of average grain size of 250 nm. The resulting cathode layer with dimensions of 3.2 × 3.2 cm^2 and active surface area of approximately 10 cm^2 has a thickness of around 35 μm.

Cell performance testing

The cell performance was evaluated in 5 × 5 cm^2 cell housing with corrugated ceramic flanges for good gas distribution. Platinum (Pt) meshes were used for current collection on both anode and cathode sides. A dead weight of 2.5 kg was placed on top of the cell housing in order to obtain better contact between the current collector and the electrodes. The anode side was flushed with humidified hydrogen with a flow rate of 500 ml min^{-1}. On the cathode side, synthetic air (20% O_2 and 80% N_2) was supplied as oxidant with a flow rate of 400 ml min^{-1} and 1600 ml min^{-1}, respectively. The current density and voltage values were recorded between 773 K and 1073 K. The impedance measurements were performed for all tested cells at a current density of 0.4 A cm^{-2} using a Solartron Schlumberger frequency response analyser (FRA) model 1255 in conjunction with a Schlumberger potentiostat model 1287A. The applied frequencies ranged from 0.01 Hz to 1 MHz with signal amplitude of 10 mV. The obtained Nyquist plots were fitted using the Zview2 fitting program. The contribution of the ohmic and electrode resistance to the total cell losses has been determined from the fit results.

Results and discussions

LSC cathode for LT-SOFCs

As has been mentioned in the introduction, the state-of-the-art cathode materials like LSM and LSCF show low catalytic activity towards oxygen reduction reaction for SOFC operated at a temperature below 973 K. Here, improved cell performance of ASC at 873 K in terms of I–V curves (Fig. 1a) and area specific resistance values subdivided in polarisation and ohmic losses (Fig. 1b) has been demonstrated when LSC cathode has been used. For comparison, the cell performance of reference ASC with state-of-the-art anode electrolyte support combined with LSCF cathode and co-fired CYO barrier layer has been included in this figure. As can be seen, a peak power density of 260 mW cm^{-2} has been obtained for the cell with the optimized LSC cathode, while 184 mW cm^{-2} was measured for the reference cell. Also the stability of the cell with LSC cathode has been tested at operating temperature for 1000 h. Less than 1 V%khr degradation rate has been observed that shows very good stability of this type of fuel cell at operating temperature of 873 K (figure is not shown here).

The impedance measurement confirm that by using LSC as cathode both ohmic and polarization resistance have been diminished (Fig. 1b). The reduction of ohmic resistance might be attributed to the fact that LSC has higher electronic and especially ionic conductivity compared to LSCF in the tested temperature regime [14–16,24,25].

Optimization of CGO diffusion barrier layer

In a second step, the electrochemical performance of the ASC with LSC cathode has been further enhanced by optimization of the CGO interdiffusion barrier layer in order to fulfil three requirements: as thin as possible, high density and sintered at temperature as low as possible. In order to investigate the influence of the layer thickness on the ohmic constitution, three ASCs have been manufactured consisting of variation in layer thickness by varying the amount of screen printed layers, followed by sintered at 1573 K for 1 h. Subsequently the cell performance test has been carried out under conditions described previously. In Fig. 2a, the I–V characteristics of the tested cells with variation of thickness of CGO layers at an operating temperature of 873 K show that the cell performance increases with decreasing CGO barrier layer thickness. The contribution of the cell losses at a current density of 0.4 A cm^{-2} has been shown in Fig. 2b. As can be seen, the ohmic resistance has the largest contribution to the decline of total cell losses. A small increase in polarization resistance along with increased CGO layer thickness has been observed. The cause of that is unclear. One possible explanation is that the manufacturing procedures of the cathodes between thin CGO layer (1 micron) and the thicker CGO layers (4 micron and 6 micron) are different, being 2 layers of screen-printed LSC cathode using a coarse screen print sieve (60 mesh) and 5 layers of screen-printed LSC layers using a fine screen print sieve (200 mesh), respectively. The use of a coarse sieve for the cathode manufacturing results in less cracks on the cathode surface and slightly thinner cathode layer compared to that using fine sieve, which might contribute to the reduction of polarization resistance. A clear relationship between the observed ohmic loss and the bi-layer electrolyte thickness (8YSZ electrolyte + CGO-layer) is shown in Fig. 3. For comparison, the theoretical correlation between calculated ohmic resistance values for the 8YSZ/CGO combination and the thickness of the bi-layer electrolyte has been included in this figure. Also the effect of the ceria layer density on this theoretical conductivity-thickness relationship is included according the given equation as followed:

$$R_{ohmic} = \frac{\left[\left(\frac{L_{8YSZ}}{\sigma_{8YSZ}}\right) + \left(\frac{L_{CGO}}{\sigma_{CGO}}\right)\right]}{A_{fract}} \quad (1)$$

Where R_{ohmic} is the area specific ohmic resistance in Ω cm^2, L_{8YSZ} and L_{CGO} are electrolyte and CGO layer thickness, σ_{8YSZ} and σ_{CGO} are the specific oxygen ionic conductivity of 8YSZ and CGO at 873 K and A_{fract} is the fractional density of the CGO layer. The fraction density of CGO layer has been determined from image analysis of SEM pictures, resulting in a value of approximately 70–75% density. As can be seen, the observed and theoretical correlation between the bi-layer electrolyte thickness and ohmic losses have different slope. The dependence of ohmic losses on the layer thickness at constant fraction density is significantly higher than the theoretically expected, which suggests that the specific oxygen ionic conductivity of this CGO/8YSZ layer combination is lower than the theoretical value. The lower observed conductivity behaviour indicates that a change in

Please cite this article in press as: Zhang-Steenwinkel Y, et al., High performance solid-oxide fuel cell: Opening windows to low temperature application, International Journal of Hydrogen Energy (2016), http://dx.doi.org/10.1016/j.ijhydene.2016.02.033

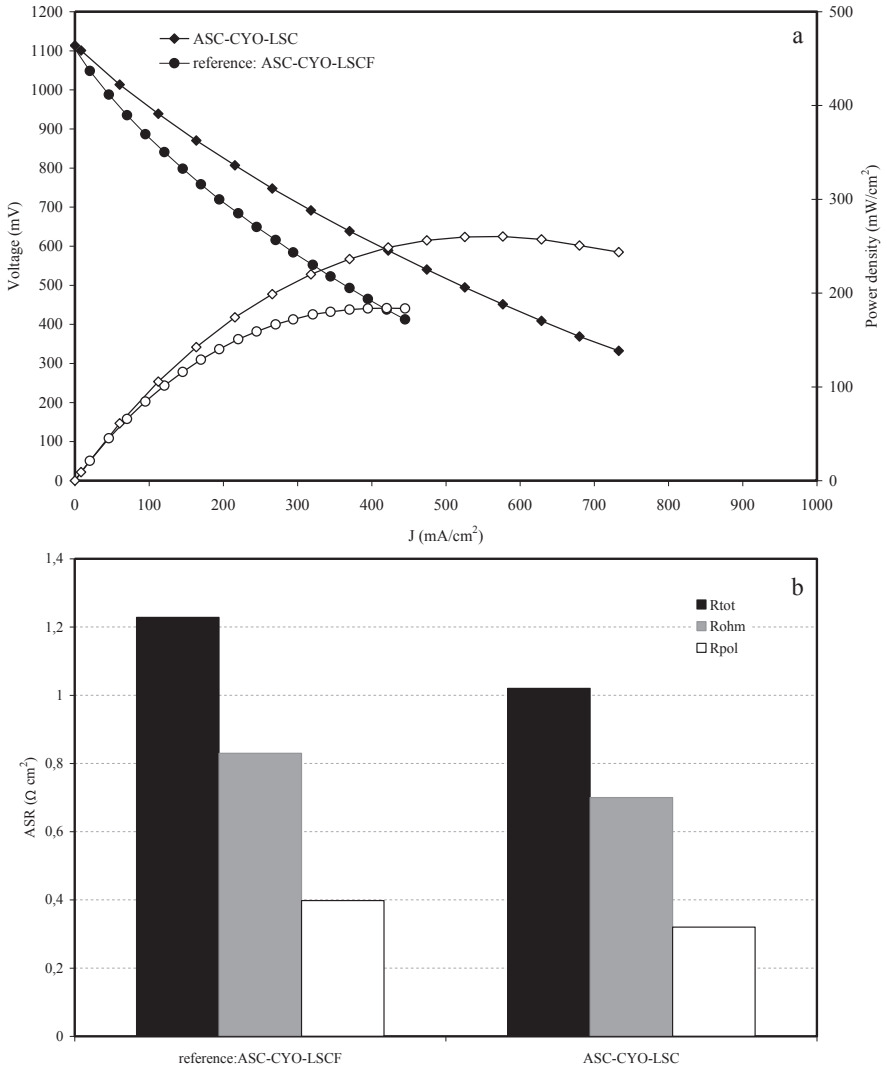


Fig. 1 – a: Cell voltage and power density as function of current density at 873 K with humidified H_2 (500 ml min^{-1}) supplied to anode and synthetic air (400 ml min^{-1} O_2 and 1600 ml min^{-1} N_2) supplied to cathode; ◆ ASC-CYO(SP)-LSC; ● reference cell: ASC-CYO(SP)-LSCF; the LSCF cathode has been sintered at 1373 K for 1 h, while the LSC cathode has been sintered at 1273 K for 1 h; b: Total area specific resistance (R_{tot}), ohmic losses (R_{ohm}) and electrode polarization losses (R_{pol}) are given for each cell configuration and has been determined by impedance measurement at 0.4 A cm^{-2} at 873 K.

composition in both layers has occurred, possibly due to the interdiffusion reaction between the zirconia and ceria layer, since these layers have been sintered at 1573 K. From the literature, it is known that the interdiffusion reaction occurs at a temperature above 1473 K [26,27]. In Fig. 3, a calculated correlation between ohmic contribution of the bi-layer 8YSZ/CGO electrolyte and thickness of the this combination has been included according to the equation given below, assuming that this bi-layer electrolyte has the same specific conductivity value as that of the single 8YSZ electrolyte at 873 K.

$$R_{ohmic} = \frac{\left(\frac{L_{8YSZ}+L_{CGO}}{\sigma_{8YSZ}}\right)}{A_{fract}} \quad (2)$$

A better match with the experimental data points has been obtained, which supports the theory that this electrolyte combination sintered at 1573 K has lower total specific oxygen ionic conductivity, compared to the theoretical expected one. The assumed interdiffusion reaction between ceria-zirconia has been confirmed by EDX-analysis of the electrolyte-barrier layer cross section (Fig. 4). An enrichment of Gd-ions at ceria-zirconia interface and a large extent of zirconium diffusion into ceria layer up to 2 micron have been observed. However, due to the formation of this interdiffusion layer, despite of its lower ionic conductivity, this layer also acts as a blocking layer to prevent the reaction between LSC cathode and zirconia electrolyte, resulting in reasonable cell performance. Ideally, in order to prevent this interdiffusion and further lowering the ohmic losses over the electrolyte bi-layer, a lower sintering temperature for the ceria layer is desirable. Moreover, this CGO-barrier layer should be dense to avoid any reaction between cathode and zirconia electrolyte. The ceria layer prepared by sputtering

Please cite this article in press as: Zhang-Steenwinkel Y, et al., High performance solid-oxide fuel cell: Opening windows to low temperature application, International Journal of Hydrogen Energy (2016), http://dx.doi.org/10.1016/j.ijhydene.2016.02.033

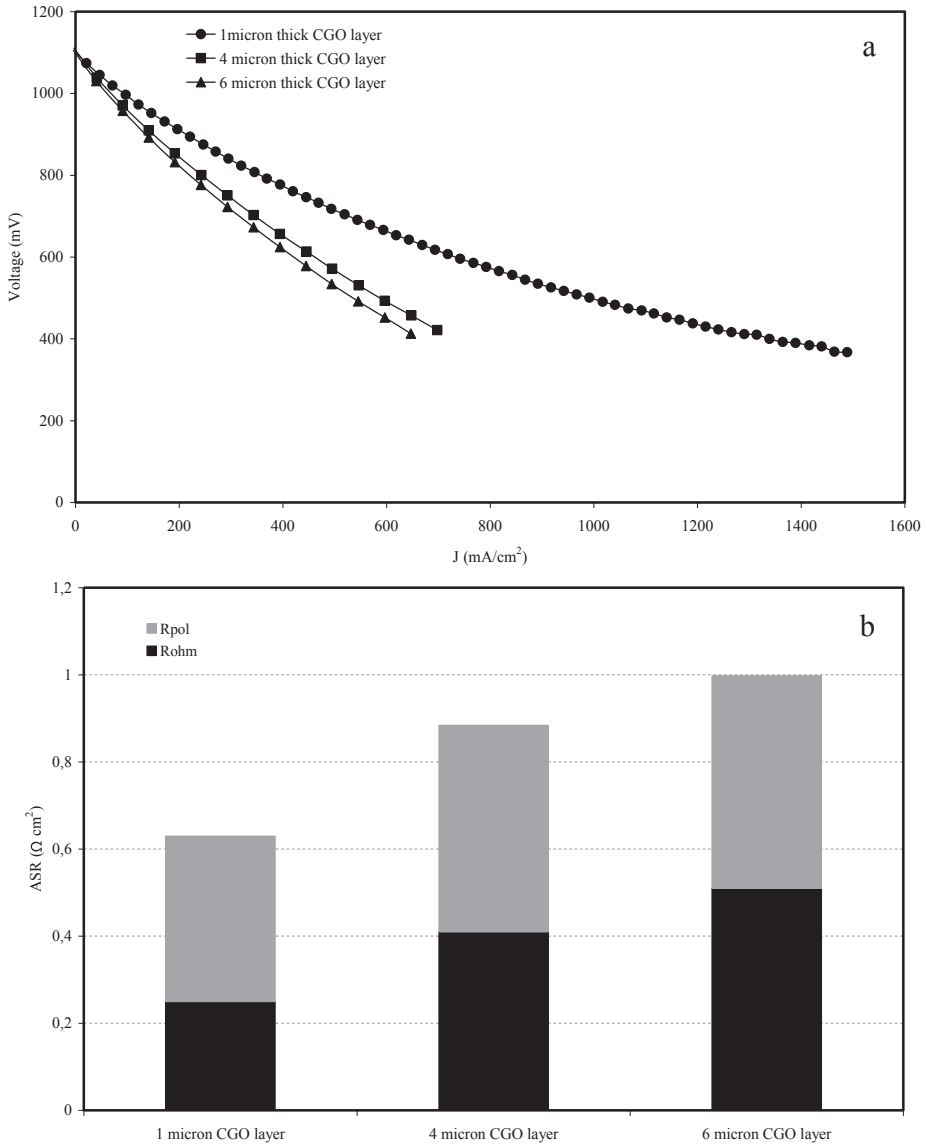


Fig. 2 – a: I–V characteristics at 873 K of anode-supported cells with screen-printed CGO layer with variation of layer thicknesses; b: The ohmic losses (R_{ohm}) and electrode polarisation losses (R_{pol}) at a current density of 0.4 A cm^{-2} and 873 K as function of ceria barrier layer thickness.

PVD technique is dense and the deposition temperature is low (see Fig. 5). For comparison, the screen-printed thin CGO-barrier layer has been included in this figure. As can be seen, this layer is thin but very porous, while the PVD-deposited CGO-barrier layer is very thin (ca. 0.3 μm) and dense. In Fig. 6a, a peak power density of 800 mW cm^{-2} was obtained for the ASC with applied sputtered CGO-barrier layer. The main improvement is due to significant diminished ohmic resistance value (Fig. 6b). The lower ohmic resistance can be attributed to the very low processing temperatures for the PVD techniques avoiding the formation of a (Ce,Gd,Zr,Y)O_2 solid solution. In addition, Uhlenbruck et al. [20] demonstrated that a dense CGO layer inhibits the $SrZrO_3$ formation due to strontium transport from the cathode to 8YSZ electrolyte, which also results in reduction of ohmic losses. The very low Ohmic resistance of the 8YSZ/PVD-CGO combination has been included in Fig. 3, which corresponds well with the theoretical expected value.

Optimization of anode substrate

The cell performance has been further improved by optimization of the anode substrate in terms of porosity and pore size distribution, aiming for improved tortuosity. The improvement in anode support morphology, in terms of tortuosity has been described in Refs. [28,29]. As can be seen in Fig. 7a, by increasing the porosity of the anode substrate from 30 to 45 vol% results in approximately 25% higher maximum power density, being 1050 mW cm^{-2} (at fuel efficiency of 50%). This improvement is the result of both diminishing ohmic and polarization losses (Fig. 7b). The reduced polarization resistance can be assigned to lower gas diffusion resistance due to the increased porosity of anode substrate. This lower gas diffusion resistance can prevent the quick downwards bending of the I–V curve at high current density. This has been demonstrated in Fig. 7a by comparing the I–V curve of the cell with low and high porosity anode substrates.

Please cite this article in press as: Zhang-Steenwinkel Y, et al., High performance solid-oxide fuel cell: Opening windows to low temperature application, International Journal of Hydrogen Energy (2016), http://dx.doi.org/10.1016/j.ijhydene.2016.02.033

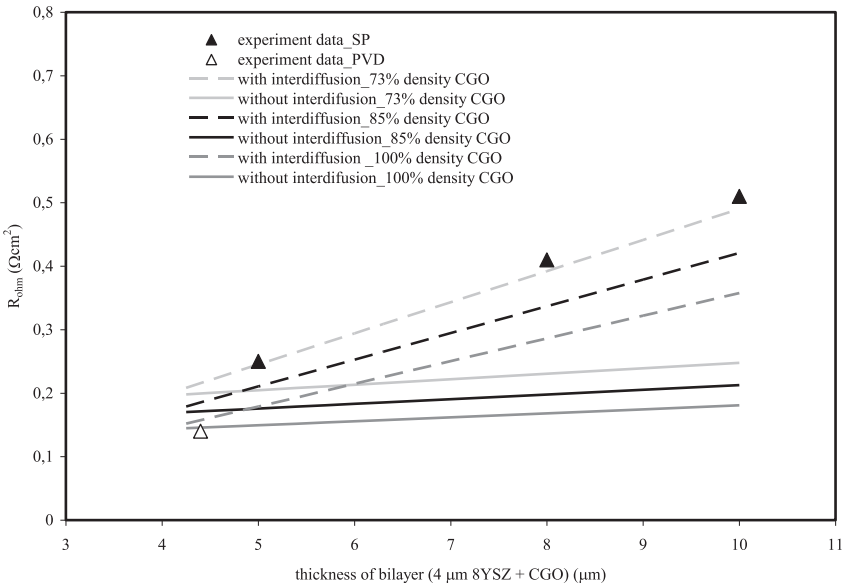


Fig. 3 – Ohmic resistance contribution to the total cell losses at 873 K as function of ceria layer thickness. The theoretical calculated R_{ohm} as function of ceria/zirconia layer thickness and ceria layer density is shown as solid lines, assuming theoretical oxygen ionic conductivity values is the sum of that of the 8YSZ- and CGO-layer. The dotted lines represent the calculated R_{ohm} as function of the bi-layer thickness and ceria layer density, assuming that the specific conductivity of this bi-layer electrolyte is equal to that of 8YSZ. Also the R_{ohm} of PVD deposited ceria layer has been included (open marker).

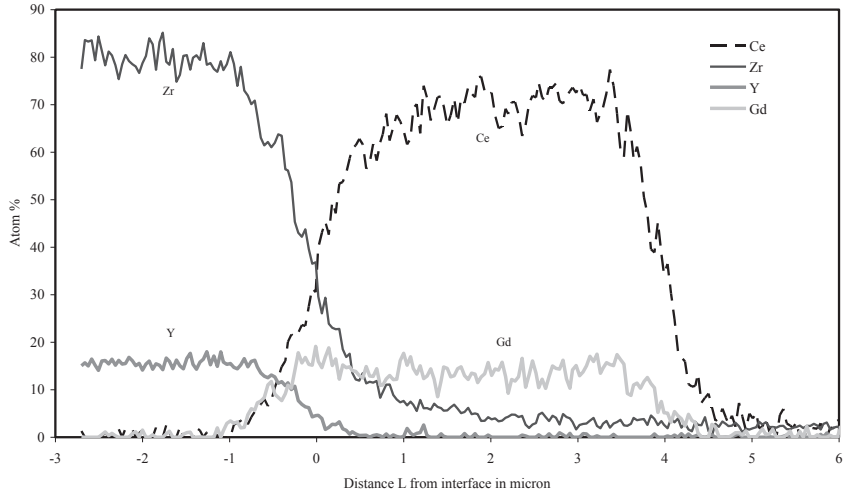


Fig. 4 – EDX-line scans of zirconia-ceria-fracture interface of ca. 4 micron thick CGO layer sample sintered at 1573 K. The negative L-values represent the position of the zirconia electrolyte and the positive L-values represent the positions of the ceria layer.

Conclusions

This paper shows that a significant improved cell performance at operating temperature of 873 K has been obtained for anode-supported cells consisting of thin film zirconia electrolyte when using hydrogen as fuel. This is mainly due to three optimization steps: (1) using LSC as cathode material; (2) implementing optimized CGO interdiffusion barrier layer aiming for thin and dense layer sintered at lower temperature; (3) improving the tortuosity of anode substrate by means of increasing the substrate porosity. It has been demonstrated that using LSC cathode with high catalytic activity for oxygen reduction along with high ionic and electronic conductivity at 873 K results in both diminished ohmic and polarization resistance. Also it has been shown that the quality of CGO-barrier layer is of importance with respect to further reducing the ohmic contribution, in particular, at high current density, since the ohmic contribution is dominant. The screen printing technique has been demonstrated to be suitable for deposition of a thin CGO layer on the electrolyte. However, this layer is still porous and has to be sintered at a temperature as high as 1573 K that results in the formation of a $(Ce,Gd,Zr,Y)O_2$ solid solution with a lower oxygen ionic

Please cite this article in press as: Zhang-Steenwinkel Y, et al., High performance solid-oxide fuel cell: Opening windows to low temperature application, International Journal of Hydrogen Energy (2016), http://dx.doi.org/10.1016/j.ijhydene.2016.02.033

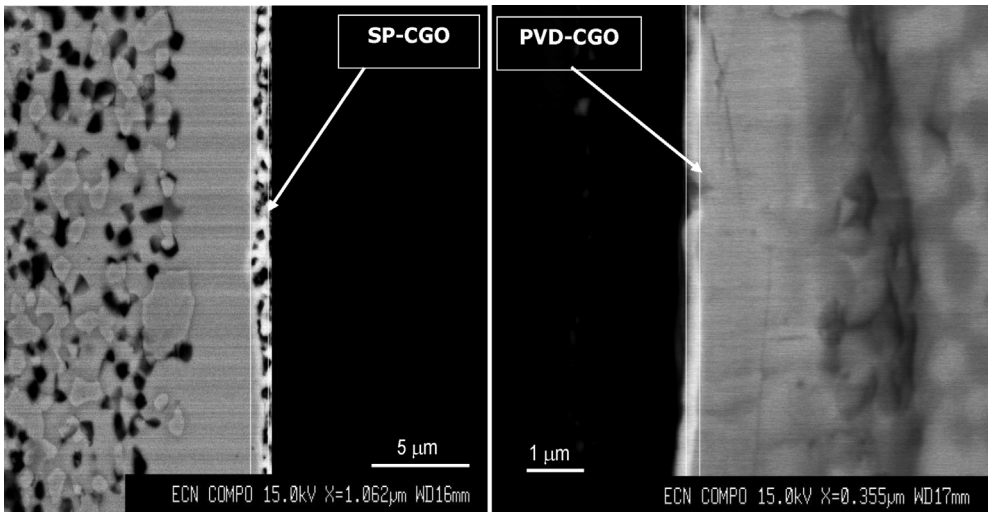


Fig. 5 – SEM images of cross sections of ASCs with CGO-barrier layers prepared by screen printing (left) and PVD (right). The CGO-barrier layers are indicated by the surrounding lines.

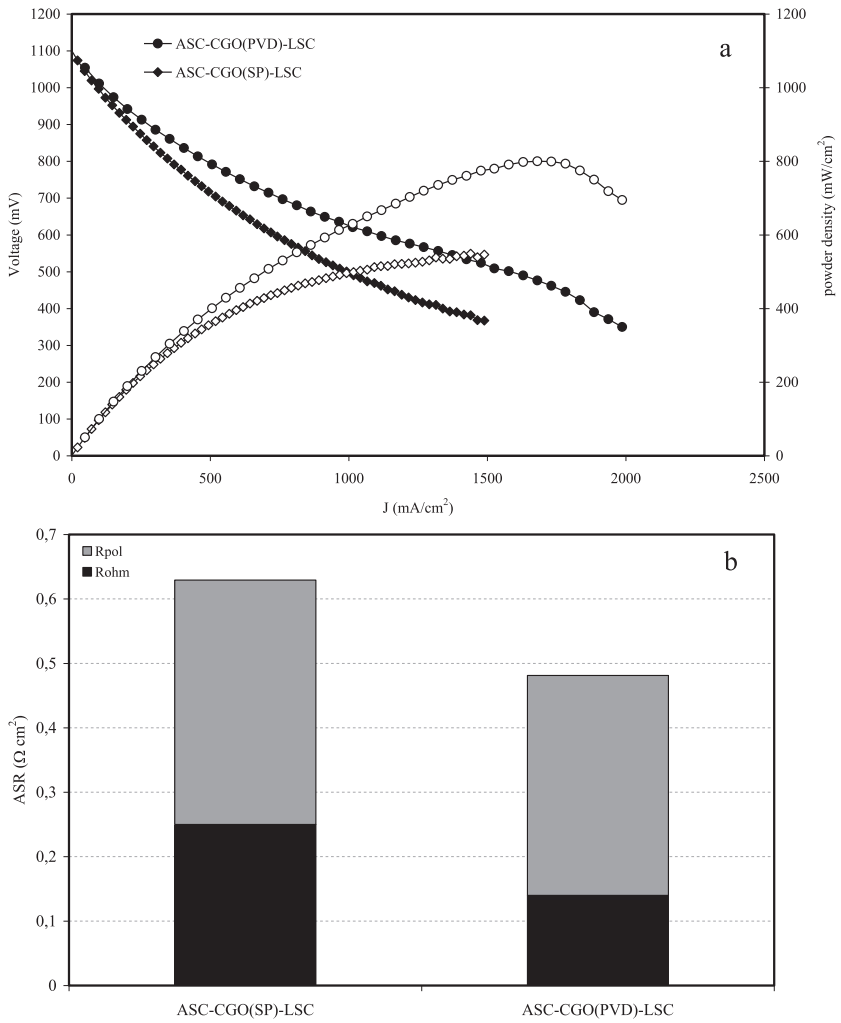


Fig. 6 – a: Cell voltage and power density as function of current density at 873 K with humidified H_2 (500 ml min^{-1}) supplied to anode and synthetic air (400 ml min^{-1} O_2 and 1600 ml min^{-1} N_2) supplied to cathode; ● ASC-CGO(PVD)-LSC; ◆ ASC-CGO(SP)-LSC; the LSC cathode has been sintered at 1273 K for 1 h; b: The ohmic losses (R_{ohm}) and electrode polarization losses (R_{pol}) are given for each cell configuration and has been determined by impedance measurement at 0.4 A cm^{-2} at 873 K.

Please cite this article in press as: Zhang-Steenwinkel Y, et al., High performance solid-oxide fuel cell: Opening windows to low temperature application, International Journal of Hydrogen Energy (2016), http://dx.doi.org/10.1016/j.ijhydene.2016.02.033

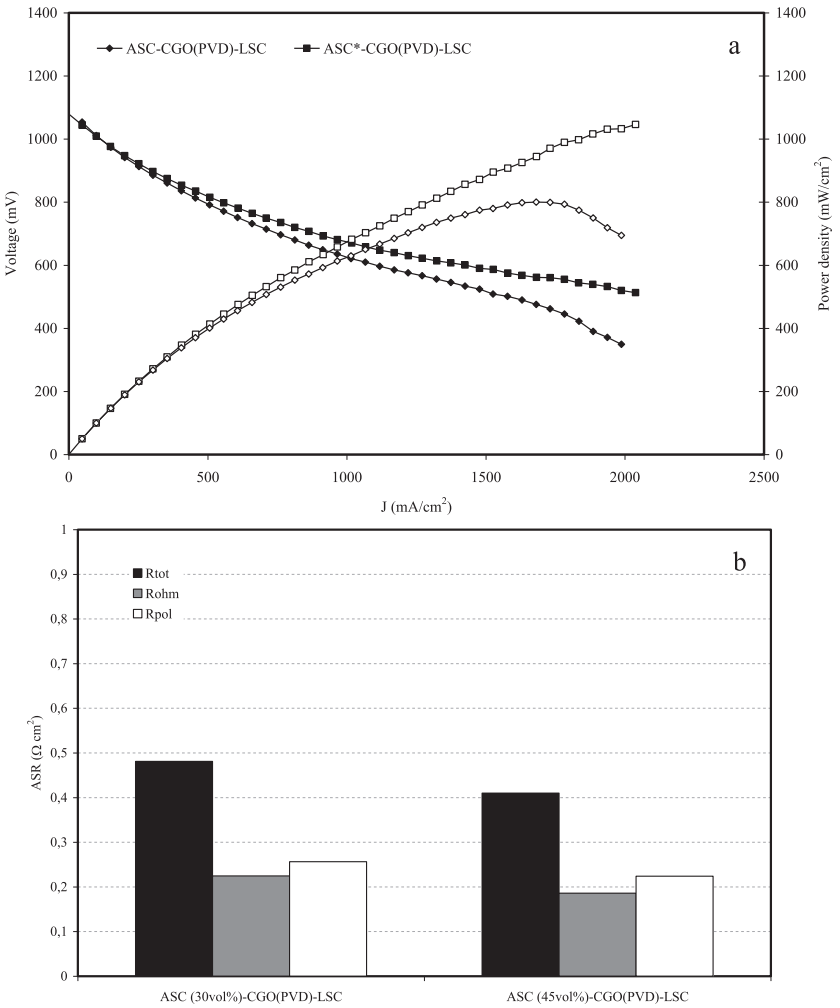


Fig. 7 – a: Cell voltage and power density as function of current density at 873 K with humidified H_2 (500 ml min^{-1}) supplied to anode and synthetic air (400 ml min^{-1} O_2 and 1600 ml min^{-1} N_2) supplied to cathode; ■ ASC*-CGO(PVD)-LSC; ◆ ASC-CGO(PVD)-LSC; the LSC cathode has been sintered at 1273 K for 1 h; ASC*: anode substrate with optimised porosity and pore size distribution; b: Total area specific resistance (R_{tot}), ohmic losses (R_{ohm}) and electrode polarization losses (R_{pol}) are given for each cell configuration and has been determined by impedance measurement at 0.4 A cm^{-2} at 873 K.

conductivity. A near perfect thin and dense CGO barrier layer has been prepared by PVD technique, leading to significant reduced ohmic resistance. Finally, further improvement in power output of the anode-supported cell has been demonstrated by the modification of the preparation process of the anode substrate by means of controlled microstructure with high substrate porosity that resulted in further reduction of both ohmic and polarization contributions.

Acknowledgements

Financial support of the European Commission is gratefully acknowledged. This work has been performed within the European project: "SOFC600" (contract no. 020089). Thanks are due to Dr. Frank Tietz and Dr. Seve Uhlenbruck (Forschungszentrum Jülich GmbH, FZJ) for providing CGO samples prepared by PVD technology).

REFERENCES

[1] Steel BCH, Angelika H. Materials for fuel-cell technologies. Nature 2001;414:345–52.
[2] Singhal SC, Kendall K. High temperature solid oxide fuel cell: fundamentals, design and application. Kidlington: Elsevier; 2003 [Chapter 1].
[3] Leng LJ, Jiang SP, Khor KA. Low-temperature SOFC with thin film GDC electrolyte prepared in situ by solid-state reaction. Solid State Ionics 2004;170:9–15.
[4] Lei Z, Zhu QS, Zhao L. Low temperature processing of interlayer free $La_{0.6}Sr_{0.4}Co_{0.2}Fe_{0.8}O_{3-\delta}$ cathodes for intermediate temperature solid oxide fuel cells. J Power Sources 2006;161:1169–75.
[5] Shao ZP, Haile SM. A high-performance cathode for the next generation of solid-oxide fuel cells. Nature 2004;431:170–3.
[6] Berkel F, Brussel Tuel M, Schoemakers G, Rietveld B, Aravind PV. Development of low temperature cathode materials. In: Kilner JA, editor. Proc. 7th European solid oxide fuel cell; 2006. P0626 (European Fuel Cell Forum, Lucerne, Switzerland).

Please cite this article in press as: Zhang-Steenwinkel Y, et al., High performance solid-oxide fuel cell: Opening windows to low temperature application, International Journal of Hydrogen Energy (2016), http://dx.doi.org/10.1016/j.ijhydene.2016.02.033

[7] Souza S, Visco SJ, Jonghe LCD. Reduced-temperature solid oxide fuel cell based on YSZ thin-film electrolyte. J Electrochem Soc 1997;144:L35–7.
[8] Jim JW, Virkar AV, Fung KZ, Metha K, Singhal SC. Polarization effects in intermediate temperature, anode-supported solid oxide fuel cell. J Electrochem Soc 1999;146:69–71.
[9] Yamahara K, Jacobson CP, Visco SJ, Zhang XF, Jonghe LCD. Thin film SOFCs with cobalt-infiltrated cathodes. Solid State Ionics 2005;176:275–9.
[10] Xu XY, Xia CG, Xiao GL, Peng DK. Fabrication and performance of functionally graded cathodes for IT-SOFCs based on doped ceria electrolytes. Solid State Ionics 2005;176:1513–20.
[11] Minh NQ, Takahashi T. Science and technology of ceramic fuel cells. Amsterdam: Elsevier; 1995. p. 117.
[12] Khan MZ, Song RH, Lee SB, Lee JW, Lim TH, Park SI. Effect of GDC interlayer on the degradation of solid oxide fuel cell cathode during accelerated current load cycling. Int J hydrogen energy 2014;39:20799–805.
[13] Zhang-Steenwinkel Y, Tuel MMA, Berkel FPF, Rietveld G. Development of novel cell components for low-temperature SOFC. EOS Trans 2007;7:271–8.
[14] Pecho O, Holzer L, Yang Z, Martynczuk J, Hocker T, Flatt R, et al. Influence of strontium-rich pore-filling phase on the performance of $La_{0.6}Sr_{0.4}CoO_{3-\delta}$ thin-film cathodes. J Power Sources 2015;274:295–303.
[15] Gwon O, Yoo S, Shin J, Kim G. Optimization of $La_{1-x}Sr_xCoO_{3-\delta}$ perovskite cathodes for intermediate temperature solid oxide fuel cells through the analysis of crystal structure and electrical properties. Int J Hydrogen Energy 2014;39:20806–11.
[16] Januschewsky J, Ahrens M, Opitz A, Kubel F, Fleig J. Optimized $La_{0.6}Sr_{0.4}CoO_{3-\delta}$ thin-film electrodes with extremely fast oxygen-reduction kinetics. Adv Funct Mater 2006;19:1–6.
[17] Yan A, Cheng M, Dong Y, Yang W, Maragou V, Song S, et al. Investigation of a $Ba_{0.5}Sr_{0.5}Co_{0.8}Fe_{0.2}O_{3-\delta}$ based cathode IT-SOFC I. The effect of CO_2 on the cell performance. Appl Cat B Environ 2006;66:64–71.
[18] Bucher E, Egger A, Caraman GB, Sitte W. Stability of the SOFC cathode material (Ba, Sr)(Co, Fe)$O_{3-\delta}$ in CO_2-containing atmospheres. J Electrochem Soc 2008;155:B1218–24.
[19] Uchida H, Arisaka S, Watanabe M. High performance electrode for medium-temperature solid oxide fuel cells La(Sr)CoO_3 cathode with ceria interlayer on zirconia electrolyte. Electrochem Solid-State Lett 1999;2:428–30.
[20] Uhlenbruck S, Jordan N, Sebold D, Buchkremer HP, Haanappel VAC, Stöver D. Thin film coating technologies of (Ce, Gd)$O_{2-\delta}$ interlayers for application in ceramic high-temperature fuel cell. Thin Solid Films 2007;515:4053–60.
[21] Jordan N, Assenmacher W, Uhlenbruck S, Haanappel VAC, Buchkremer HP, Stöver D, et al. $Ce_{0.8}Gd_{0.2}O_{2-\delta}$ protecting layers manufactured by physical vapour deposition for IT-SOFC. Solid State Ionics 2008;179:919–23.
[22] Kim SD, Moon H, Hyun SH, Moon J, Kim J, Lee HW. Ni-YSZ cermet anode fabricated from NiO-YSZ composite powder for high-performance and durability of solid oxide fuel cells. Solid State Ionics 2007;178:1304–9.
[23] Basu R, Sharma A, Dutta A, Mukhopadhyay J. Processing of high-performance anode-supported planar solid oxide fuel cell. Int J Hydrogen Energy 2008;33:5748–57.
[24] Petrov AN, Kononchuk OF, Andreev AV, Cherepanov VA, Kofstad P. Crystal structure, electrical and magnetic properties of $La_{1-x}Sr_xCoO_{3-y}$. Solid State Ionics 1995;80:189–99.
[25] Tai LW, Nasrallah MM, Anderson HU, Sparlin DM, Sehlin SR. Structure and electrical properties of $La_{1-x}Sr_xCo_{1-y}Fe_yO_3$. Part 2. The system $La_{1-x}Sr_xCo_{0.2}Fe_{0.8}O_{3-\delta}$. Solid state ionics 1995;76:273–83.
[26] Tsoga A, Naoumidis A, Stöver D. Total electrical conductivity and defect structure of ZrO_2–CeO_2–Y_2O_3–Gd_2O_3 solid solutions. Solid State Ionics 2000;135:403–9.
[27] Sammes N, Tompsett G, Cai Z. The chemical reaction between ceria and fully stabilised zirconia. Solid State Ionics 1999;121:121–5.
[28] Berkel F, Berkeveld L, Nammensma P, Hofmann P, Panopoulos KD, Ouweltjes JP. Performance improvement of anode supported cell by optimisation of anode substrate porosity. In: Steinberger-Wilckens R, editor. Proc. 8th European solid oxide fuel cell; 2008. A0507 (European Fuel Cell Forum, Lucerne, Switzerland).
[29] Zheng K, Zhang Y, Li L, Ni M. On the tortuosity factor of solid phase in solid oxide fuel cell electrodes. Int J Hydrogen Energy 2015;40:665–9.

Please cite this article in press as: Zhang-Steenwinkel Y, et al., High performance solid-oxide fuel cell: Opening windows to low temperature application, International Journal of Hydrogen Energy (2016), http://dx.doi.org/10.1016/j.ijhydene.2016.02.033